Modeling Tools for Drilling, Reservoir Navigation, and Formation Evaluation

Sushant DUTTA
Fei LE
Alexandre BESPALOV
Arcady REIDERMAN
Michael RABINOVICH
Drilling & Evaluation Research, Baker Hughes, 2001 Rankin Road,
Houston, TX 77073, USA

ABSTRACT

The oil and gas industry routinely uses borehole tools for measuring or logging rock and fluid properties of geologic formations to locate hydrocarbons and maximize their production. Pore fluids in formations of interest are usually hydrocarbons or water. Resistivity logging is based on the fact that oil and gas have a substantially higher resistivity than water. The first resistivity log was acquired in 1927, and resistivity logging is still the foremost measurement used for drilling and evaluation. However, the acquisition and interpretation of resistivity logging data has grown in complexity over the years.

Resistivity logging tools operate in a wide range of frequencies (from DC to GHz) and encounter extremely high (several orders of magnitude) conductivity contrast between the metal mandrel of the tool and the geologic formation. Typical challenges include arbitrary angles of tool inclination, full tensor electric and magnetic field measurements, and interpretation of complicated anisotropic formation properties. These challenges combine to form some of the most intractable computational electromagnetic problems in the world. Reliable, fast, and convenient numerical modeling of logging tool responses is critical for tool design, sensor optimization, virtual prototyping, and log data inversion. This spectrum of applications necessitates both depth and breadth of modeling software—from blazing fast one-dimensional (1-D) modeling codes to advanced three-dimensional (3-D) modeling software, and from in-house developed codes to commercial modeling packages.

In this paper, with the help of several examples, we demonstrate our approach for using different modeling software to address different drilling and evaluation applications. In one example, fast 1-D modeling provides proactive geosteering information from a deep-reading azimuthal propagation resistivity measurement. In the second example, a 3-D model with multiple vertical resistive fractures successfully explains the unusual curve separations of an array laterolog tool in a shale-gas formation. The third example uses two-dimensional (2-D) and 3-D modeling to prove the efficacy of a new borehole technology for reservoir monitoring.

Keywords: Modeling, oil and gas, reservoir navigation, formation evaluation, array laterolog, reservoir monitoring, transient electromagnetics

1. INTRODUCTION

Borehole tools are routinely used in the oil and gas industry to measure rock and fluid properties in and around the wellbore. This branch of the oil and gas industry is called well logging. Well logging tools that perform measurements while the well is being drilled are called logging-while-drilling (LWD) tools, while those that perform measurements after the well has been drilled are called wireline tools. The foremost application of LWD tools is reservoir navigation, which is the matching of geological and other physical models to drill along and through bed boundaries to precisely place wells. The primary application of wireline tools, as well as another important application of LWD tools, is formation evaluation, which is the process of interpreting a combination of measurements taken inside the wellbore to detect and quantify oil and gas reserves and production potential in the rock adjacent to the well. The data from these measurements are usually organized and interpreted by depth and represented on a graph called a log.

Borehole logging tools can be categorized based on the tool physics and application as electrical resistivity tools, nuclear tools, nuclear magnetic resonance (NMR) tools, and acoustic tools. This paper deals with resistivity tools. The first electrical resistivity log was acquired in 1927, and today resistivity remains the most important rock property to the oil and gas industry. Pore fluids in geological formations of interest are usually hydrocarbons or water. Oil and gas have a substantially higher electrical resistivity compared to water. Hence the resistivity of a geological formation, taken in the right context, is a clear indicator of the hydrocarbon content as well as the lithostratigraphy of the formation.

Reliable, fast, and convenient numerical modeling of tool responses is critical for tool design, sensor optimization, virtual prototyping, and log data inversion. Over the years, the acquisition and interpretation of resistivity data has grown in complexity and it has become increasingly difficult to develop and use a single modeling package for all applications. This paper describes our modeling philosophy for different resistivity tools and applications. The rest of this paper is organized as follows. Section 2 describes the physics of different types of resistivity tools and general modeling principles for resistivity tools. Section 3 presents three case studies that belong to different applications and follow different modeling methods. In the first example, fast one-dimensional (1-D) modeling provides proactive geosteering information from a deep-reading azimuthal propagation resistivity measurement. In the second example, a three-dimensional (3-D) model with multiple vertical resistive fractures successfully explains the unusual curve separations of an array laterolog tool in a shale-gas formation. The third example uses two-dimensional (2-D) and 3-D modeling to prove the efficacy of a new borehole technology for reservoir monitoring.

Section 4 discusses our modeling philosophy and concludes the paper.

2. PHYSICS OF RESISTIVITY TOOLS

Before discussing tool physics, it is pertinent to introduce typical scenarios in which resistivity tools operate and which affect tool physics and measurements. The wellbore is filled with drilling fluid (also called drilling mud) while the well is being drilled. The drilling fluid could be water-based (conductive) or oil-based (resistive). With time, the drilling fluid typically invades the formation close to the wellbore, especially if the formation is permeable, and leaves a layer of solid residue (called mud cake) on the borehole wall. This tends to affect resistivity measurements, especially in the case of wireline logging which is usually performed hours after the well is drilled. For some resistivity tools, the eccentricity of the tool in the wellbore affects the measurements. Nearby bed boundaries with resistivity contrasts can make the interpretation of resistivity data problematic. Similarly, anisotropy in the formation can lead to misleading measurements.

In general, all resistivity tools generate electromagnetic fields which obey Maxwells equations:

$$\nabla \times \mathbf{H} = \mathbf{J}_f + \frac{\partial \mathbf{D}}{\partial t} \tag{1}$$

$$\nabla \times \mathbf{E} = -\frac{\partial \mathbf{B}}{\partial t} \tag{2}$$

$$\nabla \cdot \mathbf{D} = \rho_f \tag{3}$$

$$\nabla \cdot \mathbf{B} = 0 \tag{4}$$

along with the following constitutive relations for anisotropic media:

$$\mathbf{D} = \boldsymbol{\epsilon} \cdot \mathbf{E} \tag{5}$$

$$\mathbf{B} = \boldsymbol{\mu} \cdot \mathbf{H} \tag{6}$$

$$\mathbf{J} = \boldsymbol{\sigma} \cdot \mathbf{E} \tag{7}$$

and interface conditions:

$$\mathbf{n} \times (\mathbf{H}_1 - \mathbf{H}_2) = \mathbf{J}_S \tag{8}$$

$$\mathbf{n} \times (\mathbf{E}_1 - \mathbf{E}_2) = \mathbf{0} \tag{9}$$

where $\mathbf{H}$ is the magnetic field intensity, $\mathbf{E}$ is the electric field intensity, $\mathbf{D}$ is the electric flux density (displacement), $\mathbf{B}$ is the magnetic flux density, $\mathbf{J}_f$ is the free electric current density, ρ_f is the free electric charge density, $\boldsymbol{\epsilon}$ is the electric permittivity, $\boldsymbol{\mu}$ is the magnetic permeability, $\boldsymbol{\sigma}$ is the electric conductivity, $\mathbf{J}_S$ is the surface current density on the interface, $\mathbf{n}$ is the normal vector to the interface. $\mathbf{J}$ is the bound current density and is given by $\mathbf{J} = \mathbf{J}_f - \mathbf{J}_e$, where $\mathbf{J}_e$ is the external current density.

Galvanic
Galvanic tools use a measurement (active) electrode to directly inject current into the formation. The injected current flows back to the tool via a return (passive) electrode. Galvanic tools usually operate on DC or low-frequency (< 10 kHz) AC. Fig. 1(a) shows a schematic diagram of a typical galvanic tool. Galvanic tools in a vertical borehole respond to resistances across horizontal bed boundaries in series. Hence they are more suited to water-based muds because the current can flow through the conductive mud

into the formation easily. Under the DC approximation, the time-variation of electromagnetic quantities is negligible and Eqs. (1) and (2) reduce to

$$\nabla \times \mathbf{H} = \mathbf{J}_e + \boldsymbol{\sigma} \cdot \mathbf{E} \tag{10}$$

$$\nabla \times \mathbf{E} = \mathbf{0} \tag{11}$$

Induction
Induction tools use a transmitter coil to generate a time-varying (usually time-harmonic with angular frequency ω) magnetic field. This magnetic field induces a time-varying electric field (and hence eddy currents) in the formation. The secondary magnetic field generated by the formation eddy currents is proportional to formation conductivity and is measured by a receiver coil. Induction tools necessarily operate on AC and are well-suited to oil-based muds. Fig. 1(b) shows a schematic diagram of a typical induction tool. An induction tool in a vertical borehole responds to resistances across horizontal bed boundaries in parallel. For the time-harmonic fields in the low-to-mid-frequency range (typically up to 400 kHz), we can assume stationary currents at every instant. Then the displacement current is negligible and Eqs. (1) and (2) reduce to

$$\nabla \times \mathbf{H} = \mathbf{J}_e + \boldsymbol{\sigma} \cdot \mathbf{E} \tag{12}$$

$$\nabla \times \mathbf{E} = -j\,\omega\,\boldsymbol{\mu} \cdot \mathbf{H} \tag{13}$$

where $j = \sqrt{-1}$.

Propagation
Propagation tools form a special class of induction tools that operate on high frequencies (400 kHz–GHz range). In this range of frequencies, the displacement current may not be negligible and there can be significant phase shift in the time-harmonic signal measured at the receiver. In fact, as the operating frequency increases in this range, we obtain another special class of tools called dielectric tools. Their operating frequencies are so high that displacement currents may dominate conduction currents, and these tools can measure permittivity as well as resistivity. For propagation resistivity tools, Eqs. (1) and (2) reduce to

$$\nabla \times \mathbf{H} = \mathbf{J}_e + \boldsymbol{\sigma} \cdot \mathbf{E} + j\,\omega\,\boldsymbol{\epsilon} \cdot \mathbf{E} \tag{14}$$

$$\nabla \times \mathbf{E} = -j\,\omega\,\boldsymbol{\mu} \cdot \mathbf{H} \tag{15}$$

Transient
Strictly speaking, transient tools are also induction tools but they are categorized separately because they are very different in theory and practice from the usual time-harmonic tools. In fact, transient tools are only used in surface geophysics and have never been used in borehole applications. Their principle of operation is as follows: (1) the transmitter is energized with a constant DC excitation until all transient effects expire; (2) the constant excitation is then abruptly cut off; (3) the abrupt cut-off is a broadband excitation which induces eddy currents in the formation that are proportional to the formation conductivity; (4) the induced eddy currents diffuse farther and become weaker over time; (5) the receiver measures the rate of change of secondary magnetic field of the formation eddy currents as a function of time. Hence transient measurements are performed in the absence of primary fields. Propagation effects are negligible in the time range of interest, and Eqs. (1) and (2) reduce to

$$\nabla \times \mathbf{H} = \mathbf{J}_e + \boldsymbol{\sigma} \cdot \mathbf{E} \tag{16}$$

$$\nabla \times \mathbf{E} = -\frac{\partial \mathbf{B}}{\partial t} \tag{17}$$

(a) Galvanic tool

(b) Induction tool
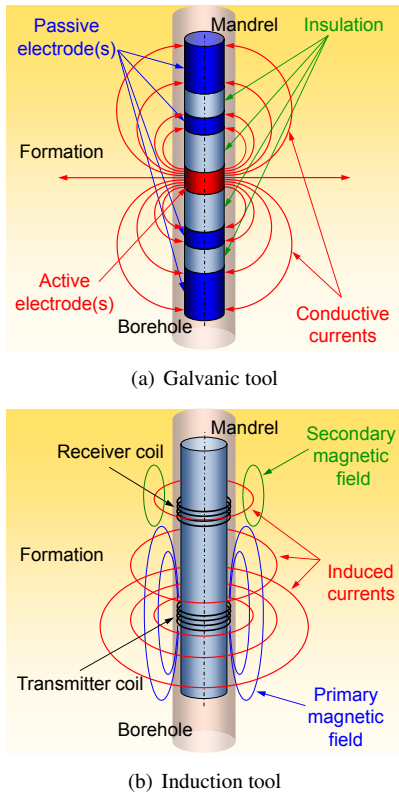
Fig. 1: Schematic diagrams of two typical kinds of resistivity tools

As seen above, resistivity tools operate in a wide range of frequencies (from DC to GHz). They obey different tool physics and impose different requirements on modeling programs. Modeling requirements are also subject to applications such as proof-of-concept studies, tool design and sensor optimization, and data inversion. Other challenges include extremely high (several orders of magnitude) conductivity contrast between the metal mandrel of the tool and the geologic formation, arbitrary angles of tool inclination, full tensor electric and magnetic field measurements, and interpretation of complicated anisotropic formation properties. These challenges combine to form some of the most intractable computational electromagnetic problems in the world. We rely on a suite of modeling programs to accomplish reliable, fast, and convenient numerical modeling of tool responses on a case-by-case basis. The numerical methods could be semi-analytical, finite-difference method (FDM), or finite-element method (FEM). In the next section, we discuss three different applications of numerical modeling of borehole resistivity tools.

3. CASE STUDIES

Geosteering
Reservoir navigation (i.e., geosteering) while drilling is a very important application area for resistivity tools. Geosteering is used to land wells at predetermined locations in a reservoir and to stay within specific regions of the reservoir to optimize the potential production of hydrocarbons. Deep-reading azimuthal propagation resistivity tools provide proactive geosteering information by indicating approaching boundaries before the wellbore actually penetrates them, thus enabling precise control of
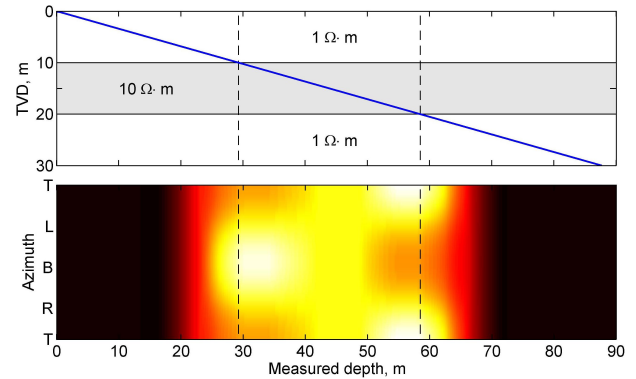
Fig. 2: Simulated deep resistivity image for a straight-line well trajectory entering and leaving a reservoir at $70°$ relative dip

the wellbore trajectory in real time [1]. Qualitative recognition of an approaching boundary and the quantitative prediction of the distance to the boundary (D2B) are both invaluable if they can be accomplished in real time.

For deep-reading propagation resistivity tools, the borehole and the volume of formation adjacent to the borehole usually do not affect the signals. Under these conditions, it is usually feasible to represent the formation and the reservoir as a layered 1-D structure with resistivity contrasts between different layers. Fast resistivity forward models are then used for pre-job planning as well as for real-time D2B inversion and geosteering along a desired well trajectory. As the formation model is relatively simple (1-D) and solution speed is imperative, the forward models consider the transmitter and receiver as point magnetic dipoles and fast semi-analytical software is used to solve forward models iteratively for real-time inversion. The metal mandrel is not implicit in the forward models, but its effect is empirically incorporated into the forward model results. Fig. 2 shows the deep resistivity image this software generated for a straight-line wellbore with $70°$ relative dip (angle made by the wellbore trajectory with the normal to the bed boundary). The top panel shows the wellbore trajectory and the 1-D layered formation model. The y-axis represents the true vertical depth (TVD) of the tool, while the x-axis represents the measured depth of the tool (the distance measured along the trajectory). The gray shaded layer is the reservoir which is ten times as resistive as the formation above and below it. The bottom panel is the deep resistivity image generated using the simulated coaxial and azimuthal propagation resistivity signals for 400 kHz frequency. The y-axis represents the borehole azimuth (T: top, B: bottom, L: left, R: right). It is clear that the propagation resistivity tool 'sees' the approaching bed boundary as much as 10 m (in terms of measured depth) away. In addition, the tool predicts whether the bed boundary is approaching the wellbore trajectory from above or below.

The information contained in deep resistivity images can help drillers to geosteer the well to their advantage [2]. Fig. 3 shows a realistic reservoir navigation case in which the well enters the reservoir and continues to be drilled at $70°$ relative dip until it reaches close to the bottom of the reservoir (as indicated by the deep resistivity image). After obtaining this good estimate of the thickness of the reservoir, the wellbore is steered up until it reaches close to the roof of the reservoir. From this point on, the trajectory is maintained at a fixed distance below the roof of the reservoir.
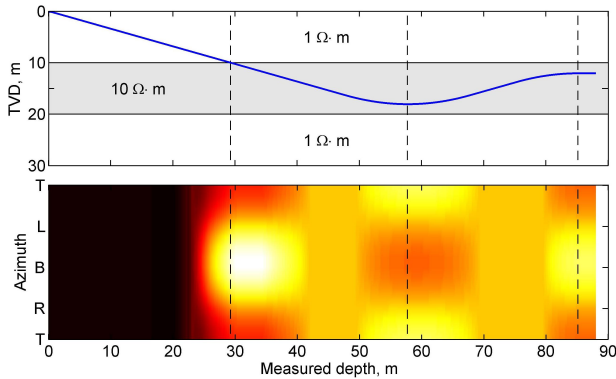
Fig. 3: Simulated deep resistivity image for a realistic geosteering scenario where the well is landed in the reservoir at 70° relative dip and then steered to stay within the reservoir close to the roof

Apart from actual signal inversion to estimate the distance to bed boundaries, these modeled deep resistivity images are also compared to deep resistivity images generated at the rig in real time to make geosteering decisions and to improve the model of the reservoir.

Array Laterolog Tool in Shale-Gas Formation

An array laterolog is a DC galvanic tool with multiple electrode spacings. The electrodes are activated in different configurations (called modes) which govern how deep the current penetrates into the formation, so that the tool yields multiple resistivity curves for different distances from the tool [3]. The distance between the tool and the region of formation being investigated is called depth of investigation (DOI). The tool measures apparent resistivity, which is the resistivity of a hypothetical homogeneous formation that would yield the same voltage-current relationship as the actual formation under investigation. In this section we describe a case study involving unusual array laterolog signals measured in numerous wells in the Bossier formation of the Haynesville shale region in Louisiana. When multiple resistivity curves obtained from galvanic or induction instruments do not coincide, this can often be attributed to the invasion of drilling fluids into the formation. The resistivity curves measured by the array laterolog in the above region also showed considerable separation, as shown in the boxed part of the resistivity log in Fig. 4 [4]. However, the Bossier formation has extremely low permeability, so that drilling fluid invasion cannot explain the curve separations. To explain the curve separations, a 3-D model with a set of parallel, vertical, gas-filled resistive fractures/thin laminations was proposed, as shown in Fig. 5.

A 3-D FEM software package is used to obtain the static solution for different electrode modes (and their corresponding DOI). Fig. 6 shows these results for different fracture and invasion cases. A single fracture across the borehole is called a drilling-induced fracture. The overlap of the red and brown curves indicates that a single drilling-induced fracture has no effect on the array laterolog response. When multiple parallel resistive fractures are introduced into the model, we see that the array laterolog modes with higher DOI show significant increase in the measured apparent resistivity, which explains the curve separations in Fig. 4.

To understand the reason for the curve separations in the array
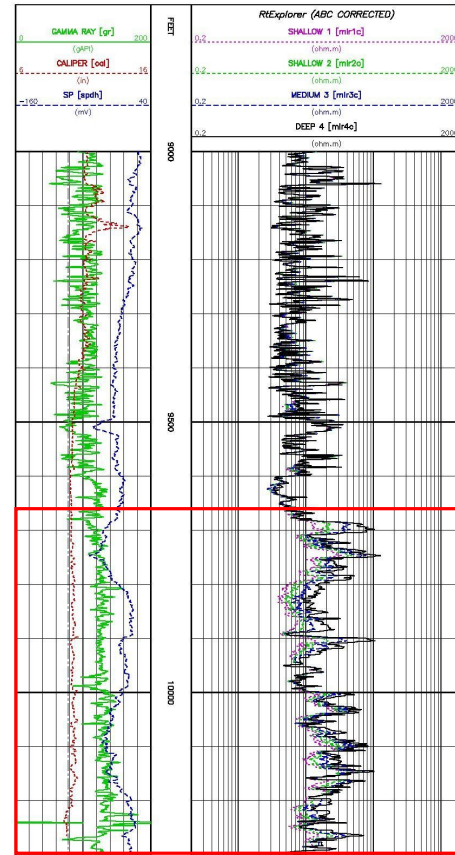
Fig. 4: Array laterolog resistivity curves logged in the upper and middle Bossier formation. Note the resistivity curve separations in the middle Bossier log response (boxed in red).

laterolog responses, the conductive current density distribution in the vertical y-z plane is plotted for the shallowest mode (DOI = 22.86 cm) and the deepest mode (DOI = 93.98 cm), as shown in Fig. 7. The activated electrodes are shown in red, while the return electrodes are shown in blue. The current distribution in the shallowest mode is not significantly affected by the fractures because the DOI of this mode is smaller than the distance of the tool from the nearest fracture. The deepest mode, in contrast, has many more electrodes activated, and the DOI is three times the inter-fracture spacing. Clearly, fractures obstruct and deform the current distribution in the deepest mode. As the DOI increases, the conduction current 'sees' an increasing number of resistive fractures, thus increasing the measured apparent resis-
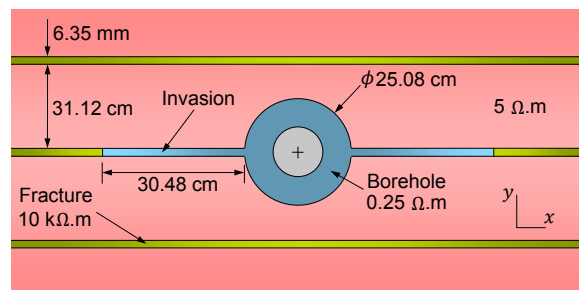
Fig. 5: 3-D model with vertical resistive fractures proposed to explain resistivity curve separations
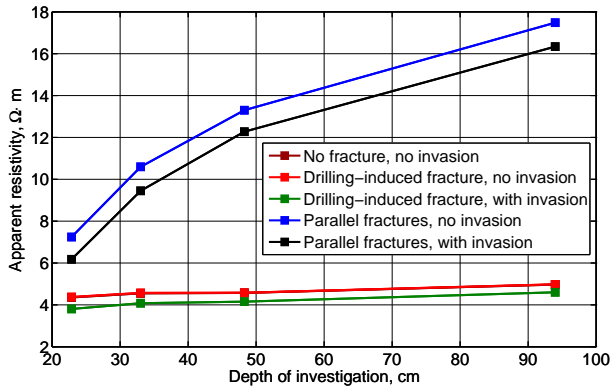
Fig. 6: Simulated array laterolog apparent resistivity as a function of DOI for different fracture and invasion cases

(a) Shallowest mode (DOI = 22.86 cm)

(b) Deepest mode (DOI = 93.98 cm)
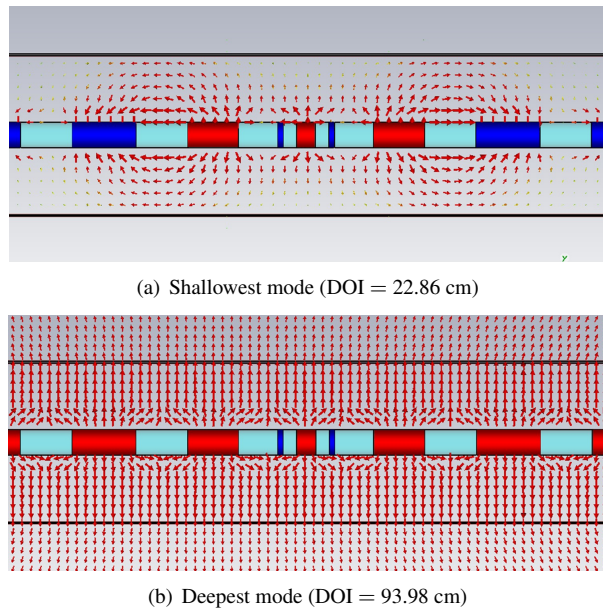
Fig. 7: Currrent density maps in y-z plane for array laterolog in formation with vertical resistive fractures

tivity.

Other simulations have indicated that, as the fracture width and inter-fracture spacing decrease, the apparent resistivity increases for each mode. In the limit of the fracture width approaching zero, the proposed fracture model resembles a uniaxially anisotropic formation with the same electrical properties in x and z directions, but different in y direction.

Reservoir Monitoring

Oil fields are very dynamic over their lifetime. As the amount of oil in a producing oil field is depleted, various techniques are implemented to exploit the oil field to the maximum and keep the production process economical. Enhanced oil recovery (EOR) processes such as waterflooding, steam flooding, and chemical flooding are extensively used all over the world to produce oil from mature oil fields. These processes involve the use of an injector well to inject water, steam, or water-based chemicals into the reservoir. The injected fluids help maintain the reservoir pressure and drive oil to the producer well. EOR processes cause key changes in reservoir fluid composition over time. Reser-
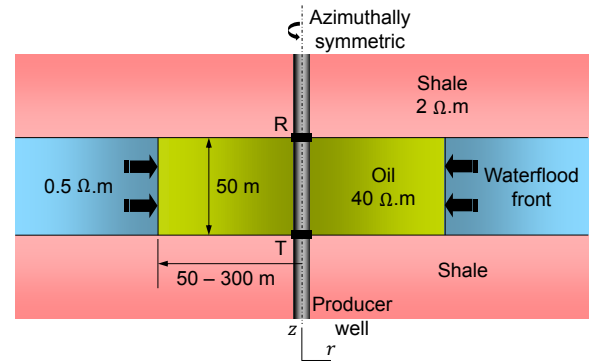
Fig. 8: Proof-of-concept model for reservoir monitoring using TEM borehole technology

voir monitoring—accurately mapping the fluid distribution and fluid dynamics at the reservoir scale—is critical for obtaining the best results from EOR processes. Reservoir monitoring is a relatively new application area for resistivity tools. Over the last twenty years, crosswell tomographic borehole electromagnetic techniques have been used for reservoir monitoring [5].

Very recently, a novel transient electromagnetic (TEM) borehole technology was applied to reservoir monitoring [6]. A 2-D FEM software was used to conduct transient simulations for initial proof-of-concept studies. Later, 3-D FEM software was used for feasibility studies. Fig. 8 shows the axisymmetric proof-of-concept model. It assumes a 50 m-thick oil reservoir with conductive shale above and below. The waterflood front is azimuthally symmetric around the borehole and advances towards the borehole with time. This is a simplification of the case where the producer well is surrounded by many equidistant and identical injector wells. The transmitter and receiver coils are placed coaxially in the producer well and point along the wellbore axis. The producer well casing is assumed to be non-conductive, at least in the region close to the transmitter and receiver, and hence neglected.

The distance between the producer wellbore and the waterflood front is denoted by D2B. Fig. 9 shows the simulated transient coaxial receiver signals for different values of D2B. The signals are calculated for unit transmitter dipole moment and unit receiver area. TEM signals are characterized by very large dynamic range, typically one to five decades of amplitude per two decades of time. It is clear from the simulations that this method is sensitive to a radial waterflood front 300 m away. After proving the concept of a borehole TEM reservoir monitoring system using 2-D axisymmetric simulations, a 3-D model was constructed for the feasibility study [6], as shown in Fig. 10. This is a more realistic model which addresses the worst-case reservoir monitoring scenario. It assumes a 10 m-thick oil reservoir with conductive shale above and below. There is only one injector well a large distance away on the right, so that the waterflood front can be assumed to be planar, and it advances towards the producer well with time. Again, the producer well casing is assumed to be non-conductive. Triaxial transmitter and receiver coils are placed in the producer well and all nine components of the voltage tensor can be calculated. Dutta *et al.* [6] have shown that measurement of the three diagonal elements of the voltage tensor (V_{xx}, V_{yy}, and V_{zz}) is the minimum requirement for determining the azimuthal location of the waterflood front.
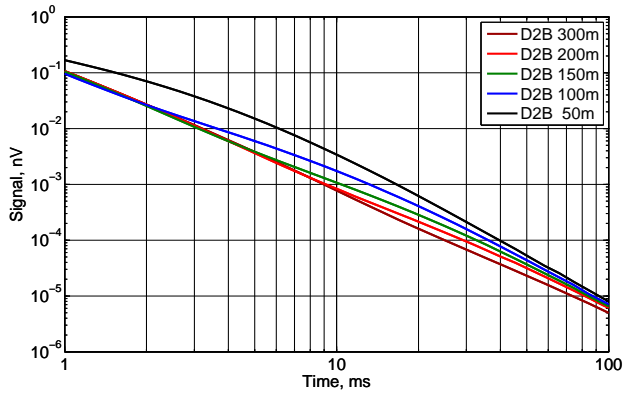
Fig. 9: Simulated coaxial receiver signals as a function of time for different distances (D2B) between the waterflood front and the producer well
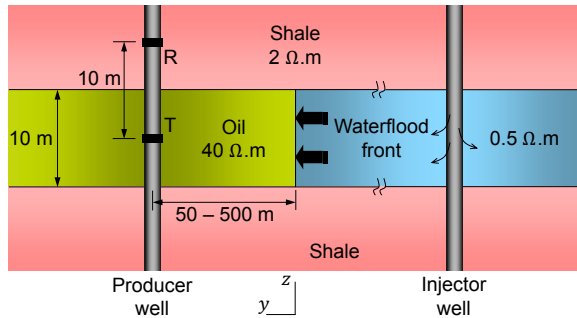
Fig. 10: 3-D model to study the feasibility of reservoir monitoring using TEM borehole technology

In this case, the reservoir is only 10 m thick (compared to 50 m thick in the 2-D model of Fig. 8). Moreover, the waterflood front approaches the borehole from only one direction. So the signals are less sensitive for the model in Fig. 10 than for the model in Fig. 8. To better visualize the signal sensitivity to the approaching waterflood front, we now consider the incremental signals $\Delta V|_{\text{D2B}} = V|_{\text{D2B}} - V|_\infty$. Fig. 11 shows the simulated incremental main component ΔV_{zz} and the incremental cross component ΔV_{zy} for different values of D2B.

It can be deduced that one must measure voltages of the order of 10^{-6} nV to resolve the waterflood front 300 m away. The signals can be improved 4–6 orders of magnitude by increasing the transmitter dipole moment and the receiver area feasibly. The signal-to-noise ratio can be improved further by techniques such as stacking and log-gating. Stacking is the averaging—simple or selective—of multiple observations (often thousands) of a noisy signal. Log-gating is a measurement technique whereby each transient signal is recorded in logarithmically increasing time-window lengths, typically 10 samples per time decade. Log-gating is particularly effective in improving the signal-to-noise ratio at late time. The above techniques yield practically measurable signals for the waterflood front 300 m away.

The above simulations demonstrate the efficacy of the TEM borehole technology proposed in [6] for reservoir monitoring. The next step in this area is to perform 3-D modeling for sensor optimization and virtual prototyping. We envision this technology will be used in a permanent sensor borehole tool, rather than a
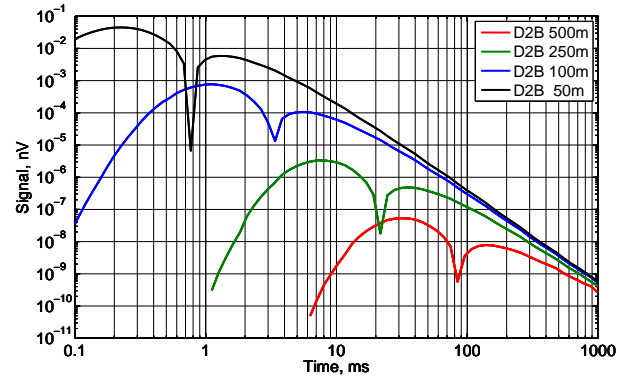
(a) Coaxial receiver
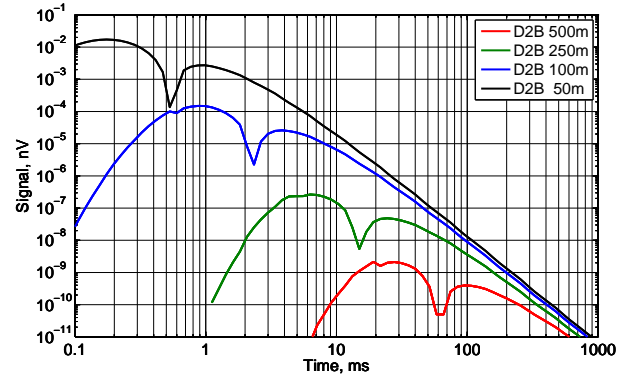
(b) Cross receiver

Fig. 11: Simulated receiver signals as a function of time for different distances (D2B)

wireline or LWD tool.

4. CONCLUSIONS

In this paper, we presented some basic concepts and applications of modeling of borehole resistivity tools used in the oil and gas industry for drilling, reservoir navigation, and formation evaluation. We discussed the basic physics of these tools, and introduced some of the challenges involved in modeling them. We described the processes and results of three very different case studies to satisfy three objectives: (1) to introduce typical resistivity tools and their usage in the oil and gas industry; (2) to outline our approach towards using different modeling software to address some of the challenges involved in modeling these tools; and (3) to describe how modeling helps us design and develop new tools.

5. ACKNOWLEDGMENTS

6. REFERENCES

[1] Bell, C., Hampson, J., Eadsforth, P., Chemali, R., Helgesen, T., Meyer, H., Peveto, C. *et al.*, "Navigating and Imaging in Complex Geology With Azimuthal Propagation Resistivity

While Drilling", Proc. of **SPE Annual Technical Conference and Exhibition**, San Antonio, Texas, USA, 24–27 September 2006, Paper 102637.

[2] Kennedy, W.D., Corley, B., Painchaud, S., Nardi, G., and Hart, E., "Geosteering Using Deep Resistivity Images from Azimuthal and Multiple Propagation Resistivity", Proc. of **SPWLA Annual Logging Symposium**, The Woodlands, Texas, USA, 21–24 June 2009.

[3] Zhou, Z., Corley, B., Khokhar, R., Maurer, H.-M., and Rabinovich, M., "A New Multi Laterolog Tool with Adaptive Borehole Correction", Proc. of **SPE Annual Technical Conference and Exhibition**, Denver, Colorado, USA, 21–24 September 2008, Paper 114704.

[4] Corley, B., Garcia, A., Maurer, H., Rabinovich, M., Zhou, Z., Dubois, P., and Shaw, N. Jr., "Study of Unusual Responses from Multiple Resistivity Tools in the Bossier Formation of the Haynesville Shale Play", Proc. of **SPE Annual Technical Conference and Exhibition**, Florence, Italy, 19–22 September 2010, Paper 134494.

[5] Mieles, L., Darnet M., Popta, J.V., Singh, M., Wilt, M., and Levesque, C., "Experience with Crosswell Electromagnetics (EM) for Waterflood Management in Oman", Proc. of **International Petroleum Technology Conference**, Doha, Qatar, 7–9 December 2009.

[6] Dutta, S.M., Reiderman, A., Schoonover, L.G., and Rabinovich, M.B., "New Transient Electromagnetic Borehole System for Reservoir Monitoring", presented at **SPWLA Topical Conference**, Abu Dhabi, UAE, 14–17 March 2011.